



Image-based decision making for reliable and proper diagnosing in NIFTI format using watermarking

Kamred Udham Singh^{1,2} · Akshay Kumar³ · Teekam Singh⁴ · Mangey Ram^{5,6} 

Received: 25 January 2021 / Revised: 28 April 2021 / Accepted: 10 January 2022 /

Published online: 29 April 2022

© The Author(s), under exclusive licence to Springer Science+Business Media, LLC, part of Springer Nature 2022

Abstract

Nowadays, advancement in Magnetic Resonance Imaging (MRI) and Computed Tomography Scan (CT-Scan) technologies have defined modern neuroimaging and drastically change the diagnosing of disease in the world healthcare system. These imaging technologies generate NIFTI (Neuroimaging Informatics Technology Initiative) images. Due to COVID-19 last several months CT-Scan has been performed on millions of the CORONA patients, so billions of the NIFTI images have been produced and communicate over the internet for the diagnosing purpose to detect the coronavirus. The communication of these medical images over the internet yielding the major problem of integrity, copyright protection, and other ethical issues for the world health care system. Another critical problem is that; is doctor diagnose the impeccable medical image of the patient because a large amount of COVID-19 patient's data

✉ Mangey Ram
dmrswami@yahoo.com

Kamred Udham Singh
kamredudhamsingh@gmail.com

Akshay Kumar
akshaykr1001@gmail.com

Teekam Singh
teekam.singh@ddn.upes.ac.in

¹ Department of Computer Science and Information Engineering, National Cheng Kung University, No. 1, University Road, Tainan 701, Taiwan

² School of Computing, Graphic Era Hill University, Dehradun, Uttarakhand, India

³ Department of Mathematics, Graphic Era Hill University, Dehradun, Uttarakhand, India

⁴ School of Computer Science, University of Petroleum & Energy Studies, Dehradun 248007 Uttarakhand, India

⁵ Department of Mathematics, Computer Science & Engineering, Graphic Era Deemed to be University, Dehradun, Uttarakhand, India

⁶ Institute of Advanced Manufacturing Technologies, Peter the Great St. Petersburg Polytechnic University, 195251 Saint Petersburg, Russia

exists. For proper diagnosing it is also necessary to identify impeccable medical image. Therefore, to address these problems a secure and robust watermarking scheme is needed for these images. Various watermarking schemes have been developed for bmp, .jpg, .png, DICOM, and other image formats but the noticeable contribution is not reported for the NIFTI images. In this paper a robust and hybrid watermarking scheme for NIFTI images based on Lifting Wavelet Transform (LWT), MSVD (Multiresolution Singular Value Decomposition) and QR factorization. The combination of LWT, QR, and MSVD helps in retaining the sensitivity of the NIFTI image and improve the robustness of the watermarking scheme. In this scheme, multiple watermarks are inserted across the first slice of the NIFTI image. The proposed watermarking scheme is sustained against various noise attacks and performance is measured in terms of PSNR, SNR, SSIM, Quality of image, and Normalized correlation. Quality of the image is much significant that lie between .99994 to .99998 and SSIM reported from .94 to .99. Whereas the PSNR of the proposed scheme lies between 56.76 to 57.28 db and NC values lie between .9993 to .9998. which shows that the results are better than the existing schemes where PSNR is lies between 32.66 to 52.02 db. Watermarking, NIFTI, MSVD, LWT, QR and Image.

Keywords Watermarking · NIFTI · MSVD · LWT · QR and Image

1 Introduction

In recent years the fast and significant advances in information technologies (IT) have grown conceptual and application-level of medical imaging. Information technologies are the backbone of fast and accurate results in medical healthcare because the medical healthcare system such as Hospital Information System (HIS) used these technologies to get fast transmission of digital medical images over the internet for the diagnosing purpose and distribution of medical data all over the world. Telediagnosis, teleconsultation, and telesurgery (e-learning of the medical staff) are the application of telemedicine where swapping of medical information is required. Medical imaging technologies such as CT-scan, MRI, Color Doppler have phenomenal contributions to the modern healthcare system. These medical modalities produce the medical image in various formats viz. DICOM, NRRD, MINC, ANALYZE, NIFT, etc. and communicate to radiologist over the internet for the diagnosing and doctors get the diagnosing result very fast and accurate in compared to film-based imaging technologies. These filmless technologies have a major advantage over film-based imaging is that many radiologists can access the same image at the same time at different places in the world and diagnose it. Filmless imaging technologies overcome the high printing cost and communication cost of these films, so film-based diagnosing shifted to filmless diagnosing. It is highly beneficial for the patient when he/she for from the doctor [34, 35]. Last some months COVID-19 spread all over the globe and affecting the social life of billions of peoples which arises the problem in front of the researchers to find the solution using digital imaging technologies to diagnose and estimation of COVID-19. But there is the main concern about the integrity and authenticity of electronic information and sensitive of medical information against malicious users and also concern the delivery of appropriate medical data too.

In the current COVID-19 situation, hospitals have a huge amount of patient's data generated by medical imaging equipment (medical images of patients) along with patient diagnosing history,

personal information, and other reports are communicated over the internet. Now it has become a common practice for various purposes like diagnosis, medical consultation, treatment, distance learning, and training, which is not enough secure. Medical practitioners viz. doctors, radiologists, and image providers do not take the security concerns seriously. Thus, at the time of medical image generation or communication, it can be intentionally or accidentally manipulated which leads to serious ramifications on the diagnosing of patient. Now a major challenge arises in front of researchers to maintain the integrity and authenticity of this sensitive medical image in an unsecured communication network. Usually, digital watermarking is suitable to ensure the authenticity and integrity of the image [6, 10, 37]. It is a technique that inserted a digital watermark (it is an image or logo which contains some meaningful information), in the host image without altering anything about the image i.e., format of image, size of the image, and keeping the data and image quality intact [30]. In the future when needed this watermark can be successfully extracted from the image to confirm the authenticity. In the medical domain, if a medical image is modified during the watermarking a breakdown in trust regarding the legitimacy of the image is generated. Any slight change in the image could provoke misdiagnosing, which prompts perilous outcomes and legitimate implications. Fundamentally, watermarking schemes are categorized as transform domain and spatial domain. In spatial domain watermarking schemes, the watermark's bits are directly embedded in the host image [17] whereas in transform domain watermarking schemes, initially, the host image is transformed into the frequency domain using the several wavelets transforms viz. LWT, DCT, DFT, DWT. Transform domain schemes are more robust than the spatial domain schemes, robustness is the main challenge for every digital watermarking technique [12, 21]. Therefore, Lifting Wavelet Transform is applied in the proposed scheme. Many authors have investigated the watermarking scheme for .tif, .png, .bmp and .jpg medical images [24, 34], or some of them have developed the watermarking schemes for DICOM medical images. In the present medical situation, numerous innovative medical imaging technologies have been industrialized which generates the NIFTI format images (.nii file extension) rather than .bmp, .jpg, DICOM (.dcm file extension) like CT-Scan, MRI etc. NIFTI images contain very sensitive medical data of the brain in form of multiple slices. So, the world medical healthcare system required a robust watermarking scheme for the authentication of the NIFTI images before the diagnosing. If watermarking scheme successful authenticate the medical image (means successful extraction of the watermark from the NIFTI image) at that point radiologist take the decision whether they go for diagnosing or not because in the present time millions of CT-Scans performed on COVID-19 patient's and transmitted over the internet. Therefore, radiologist get away to waste their time on imprecise medical data for diagnosing. Proposed watermarking scheme accomplished this and might be utilized in this corona pandemic to authenticate the NIFTI images for appropriate diagnosing.

In this scheme, initially apply the LWT on the image, which decomposes the image into four sub-bands (like LH, HL, LL, and HH). Select the LL band and applied the MSVD which decomposed the image into four bands LH, HL, LL, and HH, and select LL to embed the QR factorized watermark because it contains most of the image's energy. The presented scheme is robust against the various noise attacks. The significant contributions of this watermarking scheme are as follows

- A novel non-blind watermarking scheme for NIFTI (CT-Scan and MRI images) images based on 2-D LWT, MSVD, and QR factorization has proposed. The combination of LWT and MSVD has provided the better robustness than existing schemes.

- It is an efficient watermarking scheme for NIFTI images, multiple watermarks are embedded into the image and extracted successfully from the watermarked image even after several kinds of attacks.
- The evaluation of the proposed scheme is performed on NIFTI (.nii format) and the significant results achieved by the proposed scheme i.e. Peak Signal-to-Noise Ratio (PSNR) from 56 db to 57.27 db, Signal-to-Noise Ratio (SNR) from 45 db to 47 db, Structural Similarity Index Measure (SSIM) from .94 to .99, the Quality of Image index is 0.99 and the Normalized Correlation is .99.

This paper is organized as follows: In Section 2 summary of some recently published study related to proposed work has been discussed in Section 2. LWT, QR, and MSVD are reviewed in Section 3 and the proposed watermarking scheme is introduced in Section 4. Experimental results and analysis of proposed work with some medical images are described in Section 5. Robustness analysis of the proposed scheme is discussed in Section 6. Finally, the conclusions are given in Section 7.

2 Related work

The remarkable advances in telemedicine applications to enrapture attention and stimulate the researchers to work for the authentication and security of digital medical imaging. Basically, medical images are extensively delegated color and grayscale. In addition, most medical instruments like CT-Scan, MRI, X-Ray, Ultrasound, etc. are frequently producing a grayscale image in numerous formats like .tiff, .png, .bmp, DICOM, and so on. Hence, the researchers give more consideration to medical imaging in view of its wide applications in the advanced medical care framework. To maintain the integrity and authenticity of these medical images several watermarking schemes have been reported in the literature. N. Lin et al. [18] initially applied DWT on the image after that QR decomposition applied on the LL band and then inserted the encrypted watermark in the first row of the R matrix. Thanki & Kothari [32] proposed a Finite ridge transform and SVD based hybrid scheme for telemedicine application and use the Arnold scrambling for watermark encryption to provide more security. This scheme is robust against jpeg compression and various noise attacks. Alshanbari [2] proposed ROI based watermarking scheme for medical images for the ownership& tamper detection. The author used the DWT and SVD for better robustness and claim that the scheme is performed well against sharpening, compression, and Rescaling. LWT and a chaotic system based a reversible watermarking scheme is proposed by Tie-Gang Gao et al. [11]. The author initially applied LWT on the non-overlapping block and then LL band select for watermark insertion and the scheme is robust against cropping and compression attacks.

Su et al. [29] presented a scheme for the color image, which is based on QR decomposition and DWT, here the author initially divided the host image into 4 X 4 non-overlapping blocks and then applied QR decomposition on each block. After that watermark is embedded in the first-row fourth column element in the matrix R and the scheme is robust against cropping, blurring, rotation, scaling, adding noise, and sharpening. R. Ni. et.al [25] applied the LWT host image and then insert the watermark in LL sub-bands where selection is based on the location of spatial tempering. In this scheme, a chaotic sequence is used to estimate the location of spatial tempering. Mehta et al. [22] proposed LWT based watermarking scheme and incorporate with QR and Lagrangian support vector regression to provide more robustness and security. In this scheme, the author initially applied the LWT on the host image then decompose the LL band into 4×4 size non-overlapping blocks.

Further, QR decomposition is performed on these blocks and watermark insertion is done in the first row of the R matrix of each of the blocks. This scheme performed good against the cropping, scaling, salt and pepper noise, and JPEG compression attacks. Chamlawi et al. [5] proposed a LWT based novel semi-fragile watermarking approach, here author insert, two watermarks i.e., authentication watermark and recovery watermark used for image recovery and authentication. They claim that the scheme is efficient and secure in the presence of JPEG compression. Zairi et al. [37] proposed a scheme based on two wavelets transform, in this scheme author used DWT, DCT, and QR decomposition for more security. Watermark insertion has been done according to its entropy values on specific blocks of the image.

Gong et al. [14] proposed a scheme based on Canny edge detection, SVD, and contourlet transform. The author initially applied the contourlet transform and then divide the low-frequency band into 4×4 non-overlapping. Furthermore, SVD is applied on these blocks which are selected by canny edge detection and watermarking is done into the matrix U. Verma et al. proposed an LWT based watermarking scheme where author applied three-level LWT then divide LH band into non-overlapping blocks and then random shuffling is performed of these blocks. After that binary watermark is embedded into these blocks. The major drawback of this scheme is that it cannot sustain against the salt and pepper noise attack, rotation. Filtering. Hence, the stability between robustness and imperceptibility is continuously a challenge within the field of medical image watermarking. Tjokorda Agung B.W et al. [34] proposed a watermarking scheme for medical images based on the least significant bit (LSB) modification technique and region of Non-Interest. Initially, the original image split into the region of Interest (ROI) and region of Non-Interest (RONI). Watermark's bits have been embedded into the LSB of NROI of the image. A hybrid watermarking scheme based on DWT, SVD and DCT proposed by Takore et al. [31]. Authors initially applied DWT and the apply the DCT and SVD on the LL band of the DWT transform. Insertion of watermark's bit has been done by the modifying the coefficients of the LL sub band. Thanki et al. (2017) [33] proposed a watermarking scheme based on DCT and Fast Discrete Curvelet Transform (FDCuT). authors initially applied FDCuT on medical image and then DCT applied over the high-frequency Curvelet coefficients of the FDCuT to find the different frequency sab bands. Finally, watermark bits are embedded in the mid-band frequency of the DCT coefficients.

Most of the research works in the area of medical image watermarking has proposed the watermarking scheme for .tiff, .bmp, DICOM and .jpg image formats. Although some researcher recommended Color Doppler images in DICOM format for watermarking but the NIFTI images have the different file structure than the DICOM. But in current medical situation, numerous imaging technologies like Ct-Scan and MRI produced the 3D images in NIFTI format instead of flat and featureless .tiff, .bmp or .jpg images. These images are much transmitted over the internet for the diagnosing purpose in this covid pandemic situation. After studying the literature, we realized that little state-of-the-art contributions are found in the earlier published research for the authentication of the NIFTI images. Keeping in mind, the importance of NIFTI images in medical health care system a watermarking scheme especially for NIFTI images generated by various modern medical equipment is proposed. These images are very sensitive images, so we cannot compromise with the quality of the image. In this scheme, multiple watermarks are embedded in a slice of the NIFTI images without degrading the quality of the original image. It is a secure and robust hybrid watermarking scheme based on LWT, MSVD, and QR factorization. To ensure the image quality various image quality metrics have been evaluated and found the significant results i.e., PSNR is between 56 to 57.5, image quality index and NC (normalized correlation) is near about one.

3 Preliminaries

This section describes the methodology used in this research. In this research Multiresolution Singular Value Decomposition (MSVD), QR Factorization and, Lifting Wavelet Transform (LWT) have been used to develop a robust and secure hybrid watermarking scheme for NIFTI images.

3.1 Lifting wavelet transform

Daubechies & Sweldens [7] proposed Lifting Wavelet Transform, in this transform construction is done in the spatial domain this is the main feature of the lifting scheme. It overcomes the limitations of the conventional wavelet transformation by decreasing the complexity of time and space (because it does not require complex mathematical calculations, unlike traditional wavelet transform). So computing wavelet transforms an efficient and most straightforward algorithm. Lifting Scheme does not rely on transforms from Fourier. Digital signals are basically a sequence of integers, but after the wavelet transform, the resultant message is a sequence of floating-point numbers as well; this hinders the possibility of a perfect or a reasonable reconstruction of the signal. A transformation algorithm should have a feasible reversible implementation. It preserves the domain of the message even after the transform i.e., it behaves as an operator, which transforms integer-based sequences again into integer-based sequence signals. Lifting scheme provides this facility that the domain of transform can be preserved (i.e., integer to integer) with better computational efficiency than the conventional wavelet transformations, making it a commonly used change in image processing [9, 19, 28]. Construction of a signal by using a lifting scheme consists of the following three steps:

- **Split** - In the split phase, the given signal $\omega(n)$ is split into non-overlapping odd $\omega_o(n)$ and even $\omega_e(n)$ sets as: $\omega_e(n) = \omega(2n)$, $\omega_o(n) = \omega(2n + 1)$
- **Predict** – In this step, odd set is predicted from even set. The polynomial components occurring are compensated in the high pass by the predict phase. So this phase is also known as high pass filtering operation phase. Now odd sets $\omega_o(n)$ are predicted using even set $\omega_e(n)$ and the difference $\phi(n)$ is produced as

$$\phi(n) = \omega_o(n) - P_r[\omega_e(n)],$$

Where $P_r[\cdot]$ is the predict operator and $\phi(n)$ is high-frequency component. $\phi(n)$ is the error between original set and the predicted value.

- **Update** - The even set $\omega_e(n)$ are updated using wavelet coefficient to calculate scaling function. In this stage, moments in low pass is also preserved. Therefore, this phase is also known as low pass filtering operation phase. By applying an update operator, $U_p[\cdot]$ the low-frequency component $L(n)$ represents a coarse approximation of the original signal $\omega(n)$ defined as

$$L(n) = \omega_e(n) + U_p[\phi(n)]$$

LWT decomposes the host image into four sub-bands viz. LLLH, HL, and HH. LL sub-band has the low-frequency components that contain most of the energy of the image and other sub-bands (LH, HL, and HH) have high-frequency components that contain less energy of the image. The LWT can be applied several times on the LL band to decomposing into sub-bands

because the LL band contains most of the energy of the image. Figure 1 shows the 2-level LWT. Here in Fig. 1(b) the blue square portion shows the LL sub band.

3.2 Theorem: QR factorization

In QR decomposition [1], a non-singular matrix of size $m \times n$.

$$A = Q.R$$

Where Q is an orthogonal matrix with size $m \times m$ and R is an upper triangular matrix. The row of Q matrix is generated by the applying Gram-Schmidt. A and Q is denoted as $A = [a_1, a_2, \dots, a_n]$ and $Q = [q_1, q_2, \dots, q_n]$ The upper triangular matrix R can be computed as:

$$[a_1, a_2, \dots, a_n] = [q_1, q_2, \dots, q_n] \begin{bmatrix} r_{11} & r_{12} & r_{1n} \\ 0 & r_{22} & r_{2n} \\ 0 & 0 & r_{nn} \end{bmatrix} \dots \dots \dots \quad (1)$$

$$R = \begin{bmatrix} \langle a_1, q_1 \rangle & \langle a_2, q_1 \rangle & \dots & \langle a_n, q_1 \rangle \\ 0 & \langle a_2, q_2 \rangle & \dots & \langle a_n, q_2 \rangle \\ \vdots & \vdots & \ddots & \vdots \\ 0 & 0 & 0 & \langle a_n, q_n \rangle \end{bmatrix}$$

For example, *A is an image block* size of 3×3 is represented as follows:

$$A = \begin{bmatrix} 11 & 21 & 31 \\ 46 & 44 & 48 \\ 56 & 84 & 97 \end{bmatrix}$$

Using Eq. (1), its matrix Q and upper triangular matrix R can be obtained.

$$Q = \begin{bmatrix} -0.1501 & 0.3296 & -0.9321 \\ -0.6276 & -0.7603 & -0.1678 \\ -0.7640 & 0.5598 & 0.3209 \end{bmatrix}$$

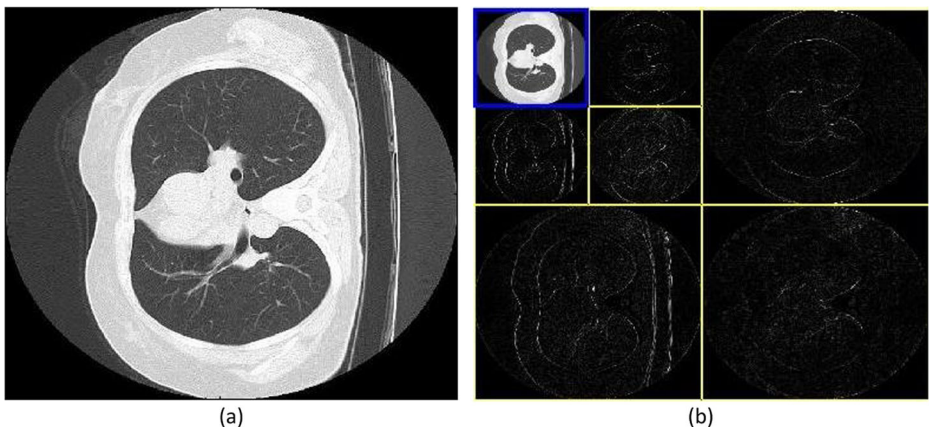


Fig. 1 2-Level LWT: (a) Original Image (b) After Applied two level LWT

$$R = \begin{bmatrix} -73.3008 & -94.9376 & -108.8802 \\ 0 & 20.4901 & 28.0219 \\ 0 & 0 & -5.8208 \end{bmatrix}$$

After multiplying both matrix Q and R, the original matrix A can be obtained.

$$Q \cdot R = A$$

$$A = \begin{bmatrix} 11.0000 & 21.0000 & 31.0000 \\ 46.0000 & 44.0000 & 48.0000 \\ 56.0000 & 84.0000 & 97.0000 \end{bmatrix}$$

3.3 Multiresolution singular value decomposition (MSVD)

MSVD basically used in real-time applications, its computational process is very simple. It doesn't have a fixed set based on vectors like Discrete Cosine Transform (DCT), Fast Fourier Transform (FFT) and Wavelet. One resolution feature is simple to distinguish, but the characteristics of multiresolution approaches are imperceptible. It is the substitution of the wavelets and is comparable to the Wavelet Multi-Resolution Analysis (MRA) since it breaks down the host picture into distinctive frequency bands (lower frequency and higher frequency LL, LH, HL and, HH) [23]. MSVD has low computational than the wavelet transformation, and directional information such as in wavelet transformations is not given. In MSVD, decomposition is based on the data set [27]. It can be utilized at many levels and deliver robustness against the various geometrical image processing attack viz. cropping, and rotation.

For a matrix, A with dimension $M \times N$, the singular value decomposition (SVD) of A into the three-matrix as shown in Eq. (2)

$$A = USV^T \quad (2)$$

Here V and U are orthonormal, and matrix S is a diagonal matrix in descending order of singular values.

MSVD for image (I) of size $M \times N$ is computed by initially reshaping I to a matrix I' of size $4 \times MN/4$. Therefore, the singular value decomposition of I' is shown in Eq. (3) as:

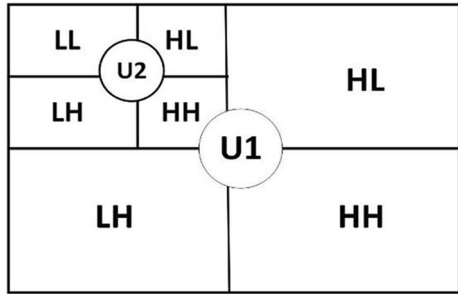
$$[U, S] = \text{SVD}(I') \quad (3)$$

Now, matrix T is shown by Eq. (4) as:

$$T = V^T I' \quad (4)$$

where matrix U of size 4×4 , matrix S of size $4 \times MN/4$ and matrix T of size $[4 \times MN/4]$. In matrix T rows I, II, III, and IV are reshaped to produce size matrices $M/2 \times M/2$. Such reformatted matrices are the image sub-bands i.e., LH, HL, LL, HH. The LL band includes the lower frequency information, and the high-frequency information is found in other sub-bands i.e., HL, LH, and HH. In this paper, we use LH band for watermarking. Figure 2 depict the structure of MSVD.

Fig. 2 Structure of Multiresolution Singular Value decomposition



4 Proposed algorithm

NIFTI images are widely used in medical imaging, as they contain metadata and a number of image slices. Watermarking of NIFTI images is a crucial task in comparison to the other image formats viz. .tiff, .png, .jpg, .bmp, DICOM, etc. The watermarking scheme must be robust and imperceptible. There must not be any noticeable modification in color, hue, and intensity, which may hamper the image's diagnosis. Metadata of the NIFTI image is exceptionally sensitive, so it must be preserved carefully. In this paper, we propose a new watermarking algorithm for NIFTI image based on MSVD, LWT, and QR factorization that incorporates the watermark embedding and extraction process.

4.1 Watermark embedding

Slices of NIFTI image and watermark both are grayscale scale. At first, metadata is put away securely from the NIFTI image, and then select the first slice for watermarking to insert the watermark. Initially apply the MSVD on this slice which breaking down it into four distinctive frequency sub-bands i.e. LL, LH, HL, and HH. Now select the HL sub-bands because it contains the most positive values. Furthermore, we apply the LWT on the HL band which decompose it into four different sub-band frequency, viz. LL, LH, HL, and HH. The LL frequency sub-band contains the vital data of the image and is resilient to the de-noising attack. Paralleling, the primary components of the watermark are subjected to QR factorization and the formation of a new vector. The augmentation of the watermark in the host slice is controlled via the scaling factor (α). Furthermore, inverse transformed (ILWT) is performed to reconstruct the slice. Finally, augment the metadata with this watermarked slice and generate the watermarked NIFTI image. The proposed algorithm is illustrated below and is also explained pictorially in Fig. 3.

Input: CT-Scan NIFTI image Size (630 X 630)

Grayscale Watermark Size (32X32) in .bmp format

Output: Watermarked NIFTI image

- Step 1 Extract metadata from the host NIFTI image and select the first slice for watermarking.
- Step 2 Perform MSVD on the selected slice that decompose it in four sub-bands LL, LH, HL and HH.

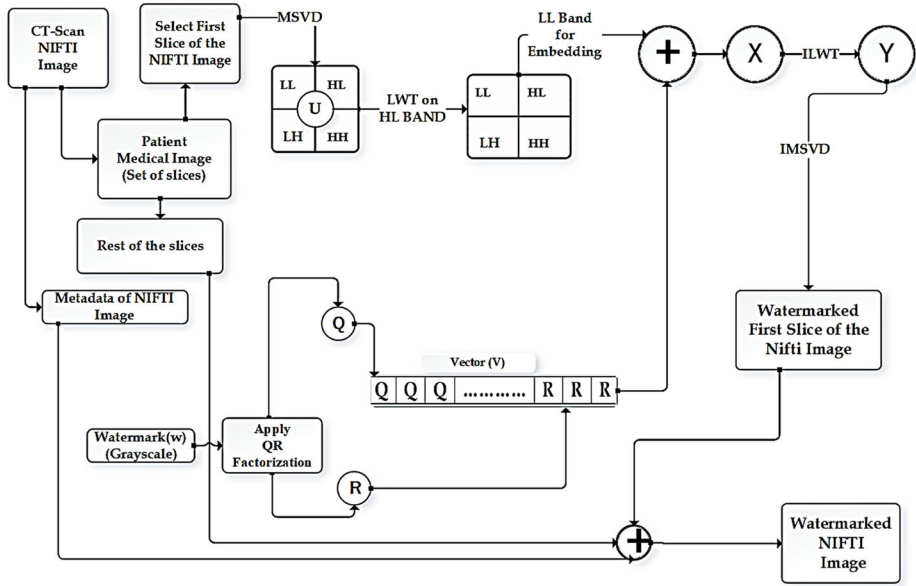


Fig. 3 Block diagram of hybrid scheme for digital watermarking process

- Step 3 Perform two-level LWT on the HL band of MSVD which decompose the image into four sub-bands LH, HL, LL, and HH
- Step 4 Apply the QR Factorization on the watermark and generate the new vector V.
- Step 5 Vector V is embedded into transformed components of the host image by selecting the LL band. Watermark is embedded in the image as below

$$x' = x + \alpha y$$

where

- x' is the transformed component of the watermark image.
- y is the factorized watermark component.
- x is the transform image of host image.
- α is the embedding strength.

- Step 6 Perform Inverse Lifting Wavelet Transformation of the final watermarked image.
- Step 7 Perform inverse Multiresolution Singular Value Decomposition on the final watermarked image.
- Step 8 Embedded the metadata in the watermarked image and generate the watermarked NIFTI image.

4.2 Watermark extraction

The watermark extraction is a crucial task of watermarking scheme; Fig. 4 depicts the watermark extraction process of the proposed watermarking scheme. It shows that the original

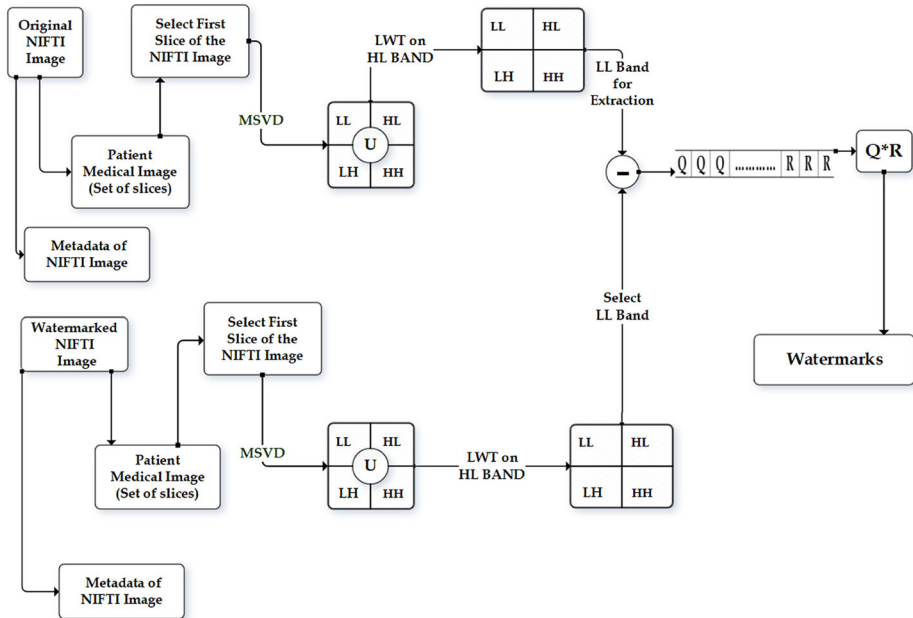


Fig. 4 Block diagram of hybrid scheme for watermark extraction

and watermarked NIFTI image is needed to separate the watermark from the watermarked NIFTI image. At first, metadata is isolated from both original and watermarked image and then select the first image slice. Furthermore, we apply the MSVD and LWT on the original and watermarked to get the embedded noisy component and afterward perform the inverse QR factorization on these noisy segments to produce the watermarks.

Input: $M \times N$ NIFTI image I ; and $M \times N$ NIFTI watermarked image I^+ .

Output: Watermark W

- Step 1 Extract metadata from both the NIFTI images i.e. I and I^+ .
- Step 2 Select the first slice of both images I and I^+ .
- Step 3 Perform MSVD on both images I and I^+ to obtain LL, LH, HL and, HH sub-bands.
- Step 4 Perform LWT on HL band of both images I and I^+ to obtain LL, LH, HL and, HH sub-bands.
- Step 5 Extract the watermark from the watermarked image using the original image by performing the reverse watermark embedding steps.

$$y = (I^+ - I)/\alpha$$

where

- I is the watermarked image.
- y is the factorized watermark component.
- I is the original image.
- α is the embedding strength.

Step 6 Perform inverse QR factorization on extracted components to get the extracted watermark.

5 Results and discussion

In this section, the results of the proposed watermarking scheme are tested over NIFTI images generated by the CT-Scan taken from public medical databases <https://zenodo.org/record/3757476#.X0pwCnkzZPZ> [20] under ethical medical practices, without revealing the patient's identity and only for the experimental purpose. The proposed watermarking scheme has been executed on the intel Core TM i7-5500U CPU 2.5 GHz Windows10 machine with 8 GB RAM on the MATLAB platform. Various NIFTI images with a resolution of 630×630 pixels and 8-bit grayscale watermark of BMP format with resolution 32×32 pixels are used for experiment.

5.1 Performance measures

The analysis of the proposed watermarking technique is verified over the ten different NIFTI images. The outcomes are investigated with respect to image quality estimations viz. PSNR (Peak Signal to Noise Ratio), MSE (Mean Square Error), NC (Normalized Correlation), SSIM (Structural Similarity Index Measure) and Q. PSNR and NC, SSIM are utilized as a measure for perceptual imperceptibility. For the watermark detectable quality assessment, PSNR is used, which is delineated as follows [16, 26, 33]:

$$MSE = \frac{1}{m*n} \sum_{i=0}^m \sum_{j=0}^n (A_{ij} - B_{ij})^2$$

$$PSNR = 10 * \log_{10} \frac{(Max)^2}{\frac{1}{m*n} \sum_{i=0}^m \sum_{j=0}^n (A_{ij} - B_{ij})^2}$$

$$SNR = 10 * \log_{10} \frac{\sum_{i=1}^n \sum_{j=1}^m (A_{ij})^2}{\sum_{i=1}^n \sum_{j=1}^m (A_{ij} - B_{ij})^2}$$

To measure the robustness of the watermarking scheme NC are utilized between the original image I and the watermarked image I^+ , if NC is near to one then the robustness of the scheme is significant. NC is evaluated using the following equation [32].

$$NC = \frac{\sum_{x=1}^M \sum_{y=1}^N w(x,y) \times w^*(x,y)}{\sum_{x=1}^M \sum_{y=1}^N w^2(x,y)}$$

Universal image quality index Q [36] is defined as follows.

$$Q = \frac{4\sigma_{xy}\bar{x}\bar{y}}{(\sigma_x^2 + \sigma_y^2) [(\bar{x})^2 + (\bar{y})^2]}$$

where, $\bar{x} = \frac{1}{N} \sum_{i=1}^N x_i$ and $\bar{y} = \frac{1}{N} \sum_{i=1}^N y_i$

$$\sigma_x^2 = \frac{1}{N-1} \sum_{i=1}^N (x_i - \bar{x})^2 \text{ (and)}$$

$$\sigma_y^2 = \frac{1}{N-1} \sum_{i=1}^N (y_i - \bar{y})^2$$

$$\sigma_{xy} = \frac{1}{N-1} \sum_{i=1}^N (x_i - \bar{x})(y_i - \bar{y})$$

$x = \{x_i | i = 1, 2, 3, \dots, N\}$ and $y = \{y_i | i = 1, 2, 3, \dots, N\}$ x and y are the original and the test image signals respectively.

Universal image quality index Q is the product of three components can be defined as:

$$Q = \frac{\sigma_{xy}}{\sigma_x \sigma_y} \times \frac{2\bar{x}\bar{y}}{(\bar{x})^2 + (\bar{y})^2} \times \frac{2\sigma_x \sigma_y}{\sigma_x^2 + \sigma_y^2}$$

Structural Similarity Index Measure (SSIM), is utilized to assess the likeness between the actual image and watermark image. SSIM value lies between -1 to $+1$, if $SSIM = 1$, at that point, original image and watermark image are exactly similar.

$$SSIM(x; y) = \frac{(2\mu_x \mu_y + c_1)(2\sigma_{xy} + c_2)}{(\mu_x^2 + \mu_y^2 + c_1)(\sigma_x^2 + \sigma_y^2 + c_2)}$$

Where μ_x : the average of actual image and μ_y : the average of watermarked image.

σ_x^2 : the variance of original cover and σ_y^2 : the variance of watermarked image with covariance σ_{xy} . Where, c_1 and c_2 are free parameters.

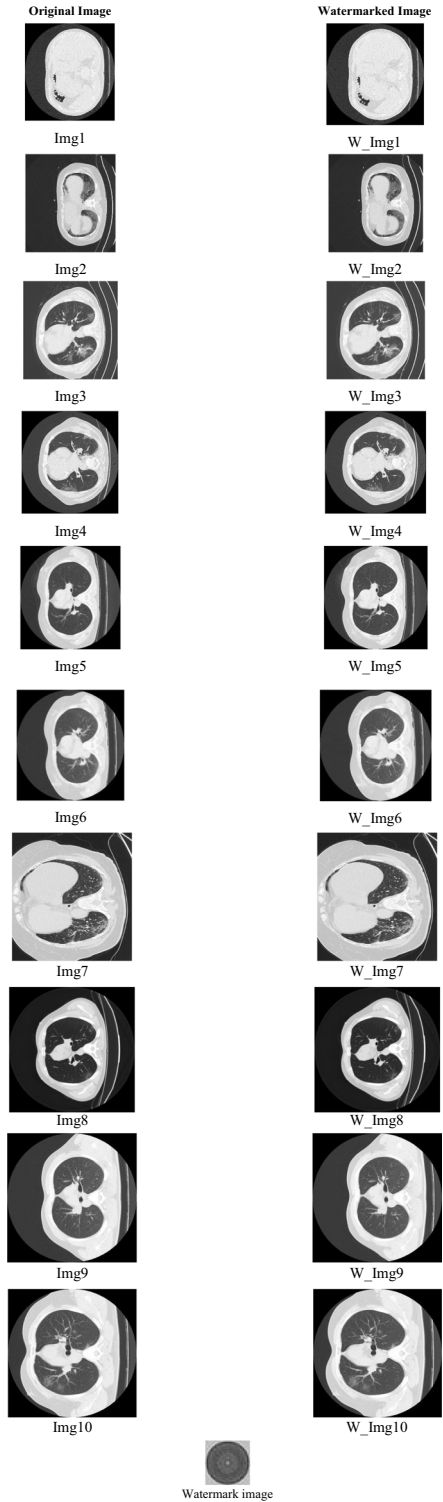
5.2 Analysis of proposed scheme

The analysis and testing of the proposed scheme has been done on ten different NIFTI images, taken from public database [20], which are *Img1*, *Img2*, *Img3*, *Img4*, *Img5* and *Img6* to determine the imperceptibility and robustness. The test results of the proposed scheme are depicted in Figs. 5 and 6. The metadata of the original NIFTI image is also preserved inside the watermarked NIFTI image.

Table 1 exhibits the performance proportions of watermarking scheme over the NIFTI images from *Img1* to *Img6*. Figure 7(a) exhibits the graphical understanding of NC between the first NIFTI image slice and watermarked image slice. Figure 7(b) & (c) shows the PSNR and SNR between the original and watermarked image respectively. Figure 7(d) speaks to the SSIM of the proposed which is more like one. Figure 8 depicts the graphical interpretation of quality measurements Q of the scheme.

Analysis of the proposed scheme has been done based on NC, SSIM and Q are having values roughly near one; that indicating excellent robustness and imperceptibility between the original and watermarked images. PSNR of the proposed scheme is more than 57 dB, which recommends that the watermarked image quality is extremely considerable.

Fig. 5 First slice of NIFTI images used for experiment and watermark image in BMP format



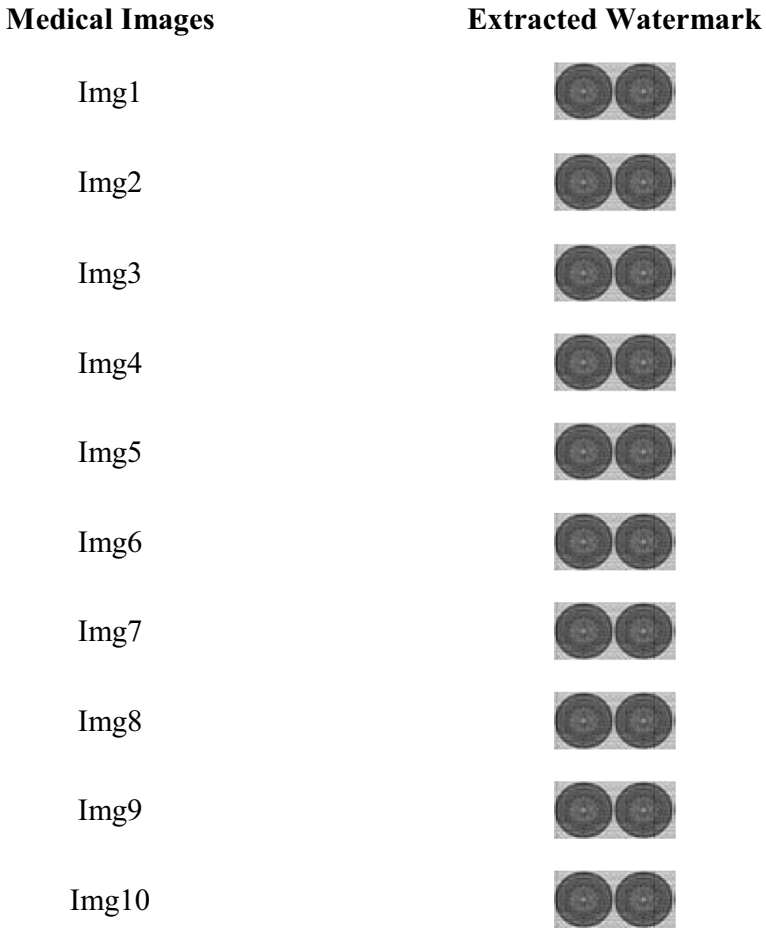


Fig. 6 Extracted watermarks from Ten medical images

Note: After successful extraction of the watermark from the received NIFTI image medical practitioners or radiologists assure that they diagnose the impeccable medical image. It is very

Table 1 Qualitative analysis of watermarked images

Medical Images	NC of Image	Q of Image	PSNR of Image	SNR of Image	SSIM	No of Watermarks
Img1	0.999798	0.999983	56.76161	46.78156	0.98547	2
Img2	0.999813	0.999976	56.92657	45.83358	0.990143	2
Img3	0.999892	0.999969	57.27539	45.99845	0.991028	2
Img4	0.999445	0.999945	57.06924	46.65178	0.946918	2
Img5	0.999681	0.999981	56.82357	47.05498	0.948062	2
Img6	0.999485	0.99998	56.98985	46.72421	0.947500	2
Img7	0.999441	0.99998	56.95649	45.75346	0.984585	2
Img8	0.999396	0.99997	57.27628	45.88567	0.978432	2
Img9	0.999623	0.99998	57.15844	46.51843	0.986248	2
Img10	0.999734	0.99997	56.92342	46.98743	0.984521	2

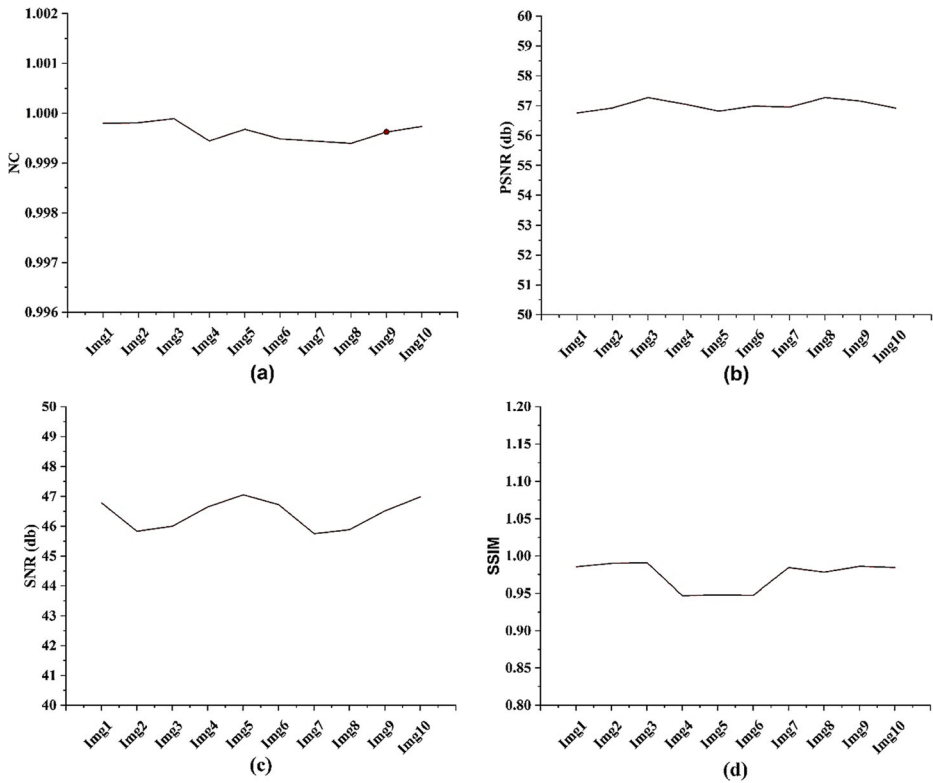


Fig. 7 Performance of Proposed Scheme for Various Medical Images: (a) Normalized Correlation (b) PSNR (c) SNR (d) SSIM measures of all ten images

important for both doctors and radiologists because it causes the life or death of a patient. Another smart role of the watermark is that it can be a logo or an image that contains some unique patient’s information such as patient id, patient name, etc. as per convenience. Therefore, this scheme may play a vital role in the authentication of the NIFTI images to produce correct diagnosing which are procreate in huge amounts due to COVID-19.

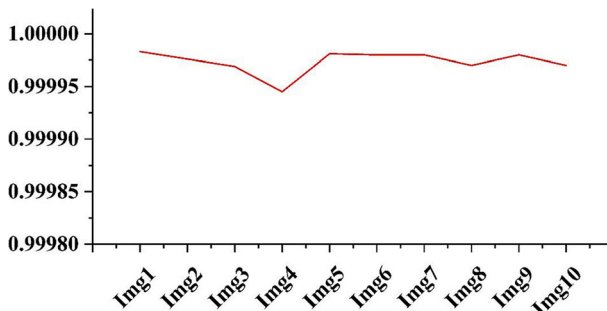


Fig. 8 Quality matrices of all ten images

5.3 Analysis of the proposed scheme for different number of watermarks insertion

The results of the proposed scheme are compared with the other existing scheme in Table 3 that the results are more. The proposed watermarking scheme embedded the different quantities of watermarks over the image slice. The most extreme watermark inclusions in the NIFTI image without hampering the diagnosis of watermarked NIFTI image exhibited in Table 2. These images contain sensitive patient's clinical data as well. In this way, it is fundamental that the nature of these images must not be debased subsequent to watermarking. This scheme is tested and analyzed with a different number of watermark addition and found that the outcomes are promising. Table 2 exhibits that the image quality measurements are legitimately relative to the quantity of watermarks addition and no noticeable change has been noticed.

Figure 9, represent the PSNR, of the proposed scheme with the different number of watermark insertion. The PSNR evaluation has been done at ten different NIFTI images. In Fig. 9 we can see that the estimation of PSNR is increased when the decreasing the number of inserted watermarks. In the event that we assess the PSNR and SNR of the img1 at 24 watermark insertions & 2 watermark insertions, there are serious variation in PSNR is 45.95 dB to 57.27 dB. Thus, if the number of watermark insertion is increased then the PSNR value will be decrease.

There is no huge difference in NC which is evaluated on ten different images. The NC results of the proposed scheme with the different number of watermark insertions are depicted in Fig. 10. The graph shows that the higher values of NC will be obtained when minimum insertion has been done in the original image. The high correlation at the two watermark insertion is 0.9999 i.e. image quality is good. But when the 24 watermarks inserted in the NIFTI image the NC value is 0.9978 which is also considerable for the scheme.

Figure 11 depicted the image quality index (Q) of the proposed watermarking scheme at the different number of watermarks insertion and reported that there is no massive difference in Q. The image quality has been evaluated on various NIFTI images, graph shows that if the number of watermarks insertion is increased the value of Q has decreased and vice versa. The value of Q is high at the minimum insertion i.e., 0.9999 and at the 24 watermarks insertion value is 0.9986 which is also good. Thus, the proposed watermarking scheme gives good results even when the number of watermark insertion is increased.

SNR is another important performance measure of the watermarking scheme. In above Figure (Fig. 12) we can see that the SNR of the proposed watermarking scheme at the different number of watermarks insertion. The SNR has been assessed on different NIFTI images, graph shows that if the number of watermarks insertion is increased the value of SNR has decreased and vice versa. The value of SNR is high at the two watermark insertion i.e., 47.10 and at the 24 watermarks insertion value is 35.95 which is likewise acceptable. Consequently, the proposed watermarking scheme gives great outcomes in any event when the quantity of watermark insertion is increased.

The results of the proposed scheme are compared with the other existing scheme (Zairi et al. [37], Takore et al. [31], BW & Permana [34], Thanki et al. [33], Hsu et al. [15], Goli & Naghsh [13], Ernawan et al. [8], Awasthi et al. [3]) in Table 3. The PSNR of proposed scheme is 56.76 to 57.28 and NC is .9993 to .9998 whereas the PSNR and NC values of other existing scheme is lies between 32.66 to 52.02. and 0.9647 to 1 respectively. Therefore, the outcomes of the proposed watermarking scheme are more significant.

The above Figure (Fig. 13) depicted the comparison of the PSNR of the proposed scheme with the other existing scheme (Zairi et al. [37], Takore et al. [31], BW & Permana [34],

Table 2 Performance verification of the proposed scheme for different number of color watermark insertion with watermark image size of 32×32

No. of Watermarks	Parameter	Img1	Img2	Img3	Img4	Img5	Img6	Img7	Img8	Img9	Img10
24	NC	0.997941	0.997928	0.997851	0.997923	0.997842	0.997857	0.99787	0.99781	0.99789	0.99791
	Q	0.998690	0.998844	0.998621	0.998721	0.998879	0.998798	0.99879	0.99876	0.99882	0.99864
	PSNR	45.98547	45.98451	45.98143	45.97991	45.98149	45.97995	45.98342	45.97362	45.97856	45.98149
	SNR	36.1479	35.99848	35.98551	36.41674	35.95718	36.43421	35.97845	35.98551	36.31628	35.96485
16	NC	0.998021	0.998752	0.998864	0.998064	0.998954	0.998038	0.99832	0.99828	0.99841	0.99865
	Q	0.999047	0.999159	0.999138	0.999058	0.999178	0.999177	0.99923	0.99919	0.99921	0.99915
	PSNR	47.75425	47.65251	47.74841	47.86587	47.45854	47.54789	47.66431	47.64876	47.86752	47.57431
	SNR	37.71864	38.16217	37.94785	37.87554	38.08713	37.97098	38.26235	37.94785	37.76526	38.29564
12	NC	0.998123	0.998764	0.998897	0.998342	0.998970	0.998351	0.99854	0.99849	0.99866	0.99875
	Q	0.999221	0.999319	0.999398	0.999433	0.999598	0.999391	0.99953	0.99949	0.99956	0.99932
	PSNR	48.83774	48.91647	48.89631	48.86657	48.97125	48.88963	48.45291	48.89872	48.96657	48.98325
	SNR	38.92147	39.75821	38.96587	38.95487	39.87417	38.97546	39.65832	38.96587	38.85349	39.94426
8	NC	0.998467	0.998841	0.998943	0.998687	0.999012	0.998558	0.99879	0.99876	0.99883	0.99886
	Q	0.999358	0.999469	0.999447	0.999685	0.999686	0.999562	0.99981	0.99974	0.99986	0.99941
	PSNR	49.84613	49.92547	49.99647	49.97584	49.99527	49.97657	49.93657	49.89773	49.87685	49.99876
	SNR	40.06542	39.95462	40.03982	40.07589	40.64187	40.95647	39.87652	40.03982	40.12495	40.59874
6	NC	0.998765	0.998976	0.999011	0.998982	0.999238	0.998908	0.99897	0.99895	0.99898	0.99899
	Q	0.999498	0.999573	0.999561	0.999812	0.999801	0.999791	0.99985	0.99982	0.99989	0.99977
	PSNR	50.97882	51.03091	51.14586	51.07362	51.08758	51.07421	51.02159	51.24685	51.27451	51.15473
	SNR	41.07548	40.99854	41.04844	41.09532	41.75249	41.96214	40.97623	41.04844	41.29492	41.79526
4	NC	0.999036	0.999114	0.999719	0.999125	0.999421	0.999125	0.99909	0.99902	0.99923	0.99935
	Q	0.999534	0.999628	0.999712	0.999948	0.999972	0.999969	0.99997	0.99995	0.99996	0.99991
	PSNR	53.18975	53.40738	53.67553	53.58336	53.65627	53.59902	53.20743	53.57687	53.48643	53.75624
	SNR	43.12137	42.91684	43.09791	43.41576	43.89273	43.99755	42.90845	43.09791	43.31486	43.95423
2	NC	0.999798	0.999813	0.999892	0.999445	0.999681	0.999485	0.99944	0.99939	0.99962	0.99973
	Q	0.999983	0.999976	0.999981	0.999945	0.999981	0.999980	0.99998	0.99997	0.99998	0.99997
	PSNR	56.76161	56.92657	57.27539	57.06924	56.82357	56.98985	56.95649	57.27628	57.15844	56.92342
	SNR	46.78156	45.83358	45.99845	46.65178	47.05498	46.72421	45.75346	45.88567	46.51843	46.98743

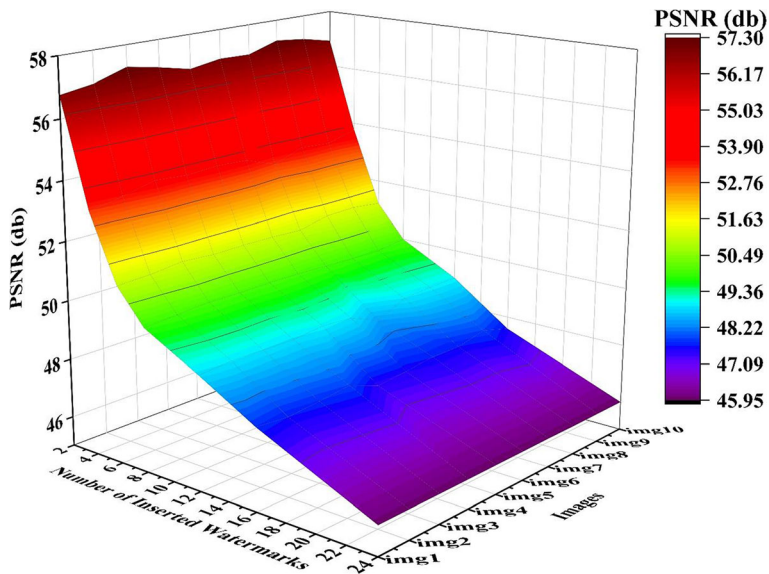


Fig. 9 PSNR comparison at different Number of Inserted Watermarks

Thanki et al. [33], Hsu et al. [15], Goli & Naghsh [13], Ernawan et al. [8], Awasthi et al. [3]). The PSNR of the proposed scheme is evaluated over the ten different NIFTI images which lie between 56.76 to 57.28 whereas the PSNR of other existing scheme is lies between 32.66 to 52.02 (PSNR of Zairi et al. [37] is 32.66 to 46.95, Takore et al. [31] is 44.52 to 44.58, BW & Permana [34] is 47.49 to 48.57, Thanki et al. [33] is 46.55 to 47.18, Hsu et al. [15] is 40.16 to 40.49, Goli & Naghsh [13] is 38.37 to 39.93, Ernawan et al. [8] is 46.11 to 47.91, Awasthi

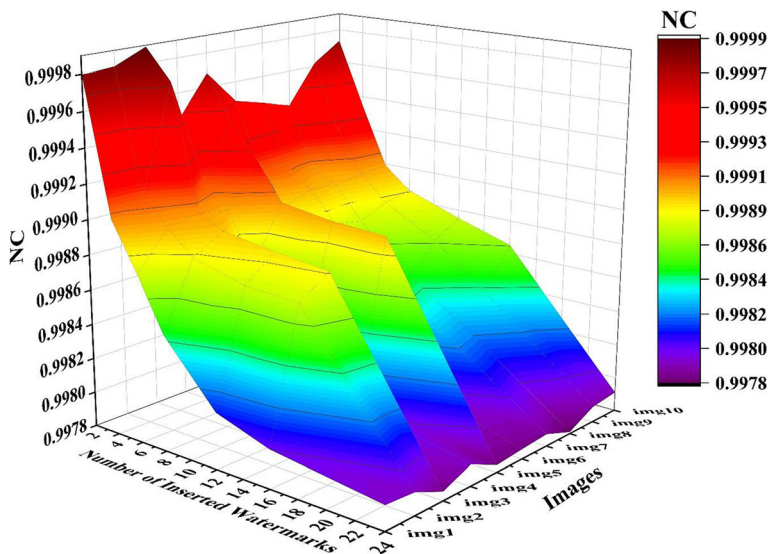


Fig. 10 Normalized Correlation comparison at different number of watermark insertion

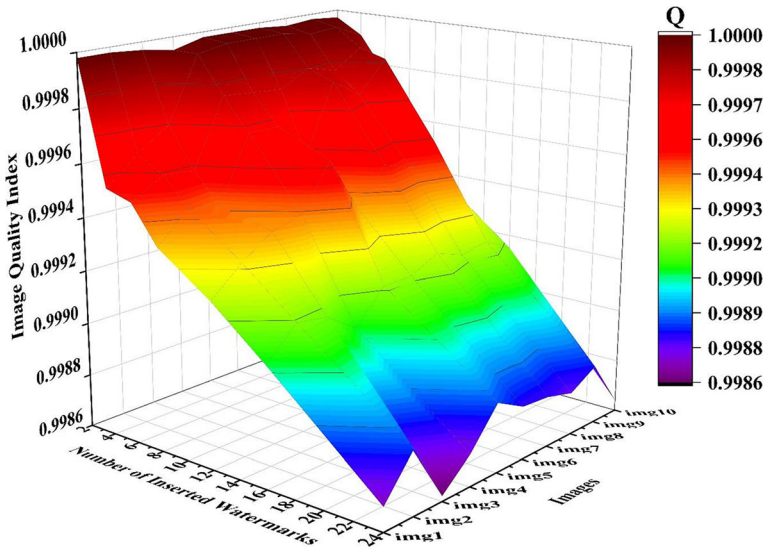


Fig. 11 Image Quality comparison at different number of watermark insertion

et al. [3] is 48.92 to 52.02. Therefore, the PSNR of the proposed watermarking scheme is more significant than the other schemes.

Figure 14 shows the comparison of the NC of the proposed scheme with the other existing scheme (Zairi et al. [37], and Thanki et al. [33]). The PSNR of the proposed scheme lies between 56.76 to 57.28 whereas the PSNR of other existing schemes is lies between .9993 to .9998 (NC of Zairi et al. [37] is 1, and the NC of Thanki et al. [33] is 0.9647to 0.9827.

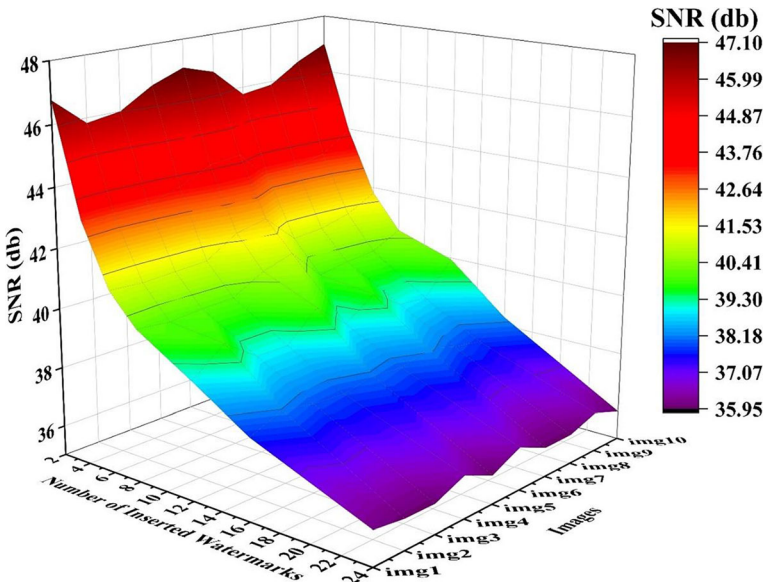


Fig. 12 SNR comparison at different number of watermark insertion

Table 3 Performance comparison of NC an PSNR values comparison between proposed and existing scheme

PSNR (db)	NC										
	Proposed Scheme (Two Grayscale watermark insertion of 32×32 size)	Zairi et al. [37]	Takore et al. [31]	BW & Permana [34]	Thanki et al. [33]	Hsu et al [15]	Goli & Naghsh [13]	Emawan et al. [8]	Awasthi et al. [3]	Proposed Scheme (Two Grayscale watermark insertion of 32×32 size)	Zairi et al. [37]
56.76161	46.959	44.5866	47.7949	47.18	40.49	38.37	47.176	50.4728459	0.999798	1	0.9827
56.97657	44.42	44.5218	47.4966	46.54	40.48	39.93	46.918	48.9276355	0.999813	1	0.9647
57.27539	32.66	44.5866	48.5741	46.55	40.16	38.74	46.116	49.7361311	0.999892	1	0.9780
57.06924	-	-	-	-	40.46	39.6	47.024	49.7085744	0.999445	-	-
56.82357	-	-	-	-	-	-	47.158	52.0171729	0.999681	-	-
56.98985	-	-	-	-	-	-	47.300	50.3163369	0.999485	-	-
56.95649	-	-	-	-	-	-	47.404	50.811477	0.999441	-	-
57.27628	-	-	-	-	-	-	47.352	49.9880453	0.999396	-	-
57.15844	-	-	-	-	-	-	47.365	-	0.999623	-	-
56.92342	-	-	-	-	-	-	47.311	-	0.999734	-	-

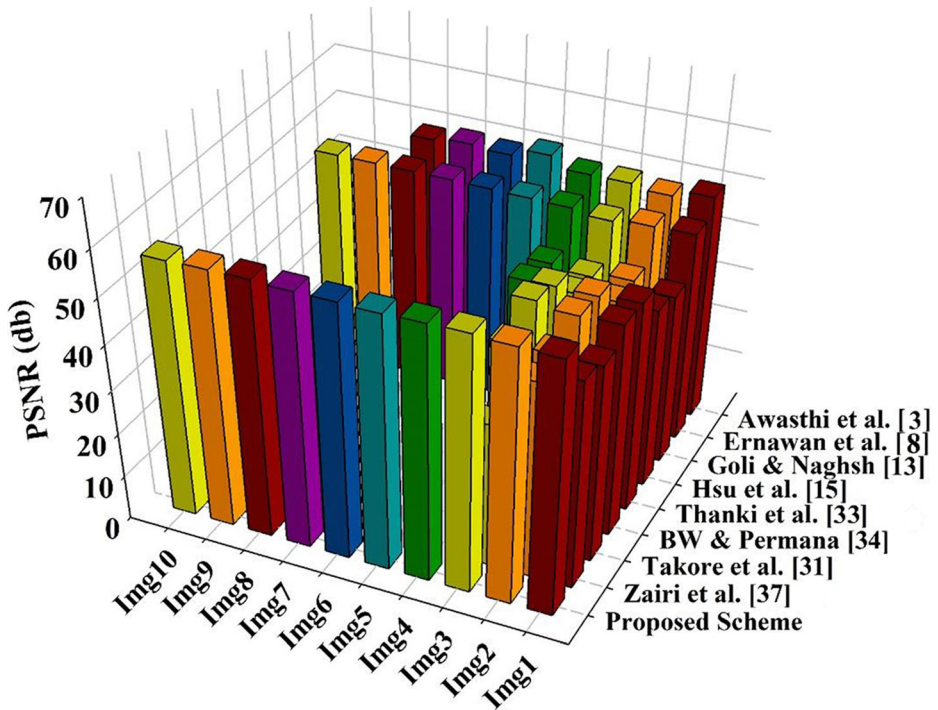


Fig. 13 Comparison of PSNR (db) Values of Proposed Scheme with Existing Schemes

Therefore, the NC of the proposed watermarking scheme is significant. After the compression of PSNR and NC values of the proposed scheme with existing schemes (Zairi et al. [37],

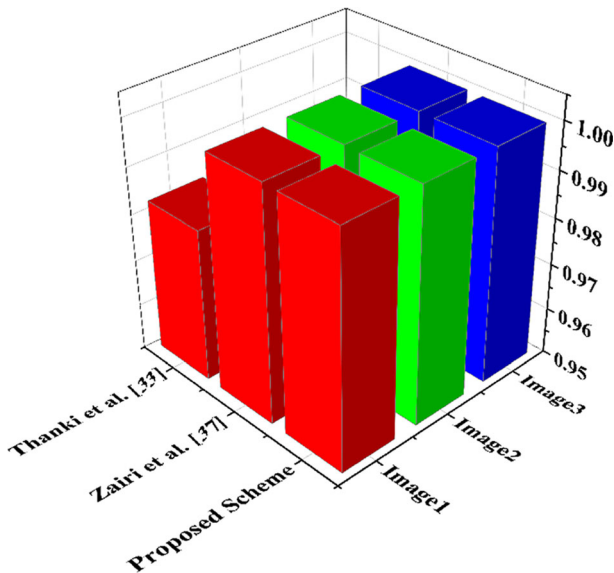


Fig. 14 Comparison of Normalized Correlation Values of Proposed Scheme with Existing Schemes

Takore et al. [31], BW & Permana [34], Thanki et al. [33], Hsu et al. [15], Goli & Naghsh [13], Emawan et al. [8], Awasthi et al. [3]) we observed that the outcomes are more significant.

6 Robustness analysis

Robustness test of proposed watermarking scheme has done, by performing the various image processing attacks viz. Salt & Pepper, Gaussian noise, Poisson, Speckle on watermarked image which may incite the clearing of watermarks. After applying the attack, if the extraction of the inserted watermark is successfully done from the altered watermarked image then the scheme is robust and legitimate in nature. A major requirement of any significant watermarking scheme is the sustenance of the scheme against these attacks. Insertion of watermarks and quality of watermarked image is inversely proportional to each other but as per the necessity, a trade-off must be considered. Subsequently, this scheme is tested with various watermarks insertion which prompts increments in robustness and degradation in image quality, but the minimum number of watermarks insertion increases the quality of the image. Various noise attacks have been applied over the watermarked image to determine the robustness of the scheme. Proposed scheme designed for CT-Scan medical image, so the diagnosis will be framed on this watermarked NIFTI image. Along these lines, any critical degradation in the watermarked image quality isn't worthy since it might cause the life and demise of the patient. Thus, the scheme is tested with the various noise attacks with the various boundaries, till the quality measurements indorse that the altered watermarked image is of high calibre.

6.1 JPEG compression

JPEG compression with quality factor 90 and 75 applied over the watermarked slice and embedded watermark extracted successfully. Table 4 depict this attack for the NIFTI images and the findings define that the efficiency of the is promising.

6.2 Salt & Pepper Noise Attack

Salt and pepper noise with noise density 0.001 to 0.004 applied on the watermarked slice of NIFTI image, and the watermark is successfully extracted. Table 5 depict that this attack for

Table 4 Parameters values of watermarked image after JPEG compression attack with quality factor 90 and 75 and extracted watermarks



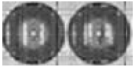



Quality Parameters	PSNR of Image	NC of Image	Extracted Watermarks
90	37.89547	0.989562	
75	32.18572	0.965417	

Table 5 Parameters values of watermarked image after Salt & pepper noise attack with variance from 0.001 to 0.004 and extracted watermarks

Noise Density	NC of Image	Q of Image	PSNR of Image	Extracted Watermarks
0.001	0.99845	0.99853	34.68754	
0.002	0.99658	0.99654	31.92548	
0.003	0.99517	0.98625	29.06416	
0.004	0.98789	0.97923	26.99728	

the slices of the NIFTI images and the findings define that the efficiency of the scheme is promising.

6.3 Speckle noise attack

Speckle noise attack applied with variance 0.001 to 0.003 on the watermarked slice of the NIFTI image and the watermark is successfully extracted by the proposed watermarking scheme. Table 6 depict the evaluation of the attack over the slice of the NIFTI image and the findings show that the result of scheme is significant.

6.4 Poisson noise attack

Poisson noise attack applied over the watermarked slice of the NIFTI image and then watermark is extracted successfully by the proposed scheme. In Table 7, analysis of the attack

Table 6 Parameters values of watermarked image after Speckle noise attack with variance from 0.001 to 0.003 and extracted watermarks

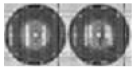


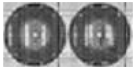
Variance	NC of Image	Q of Image	PSNR of Image	Extracted Watermarks
0.001	0.99784	0.99734	36.5476	
0.002	0.99695	0.99552	32.4254	
0.003	0.99492	0.99454	31.7451	

Table 7 Parameters values of watermarked image after Poisson noise attack and extracted watermarks

NC of Image	Q of Image	PSNR of Image	Extracted Watermarks
0.99452	0.99721	43.5472	

for the NIFTI images are tabulated and the results show that the performance of proposed scheme is favourable.





6.5 Gaussian noise attack

Gaussian noise attack applied with variance 0.001 and varying it from 0.001 to 0.004 on the watermarked slice of the NIFTI image. After the attack extraction of watermark is successful. In Table 8, analysis of the attack for the slice of NIFTI images are tabulated and the results show that the performance of proposed scheme for NIFTI images is promising.

7 Conclusions

In this paper, a novel non-blind watermarking scheme based on LWT, QR, and MSVD for NIFTI images is proposed. These images have delicate clinical image data, so the watermarking of these images is a very crucial task. For the experimental purpose we have used NIFTI images (630×630) sourced from CT-Scan and grayscale watermark (32×32). The obtained outcomes of the measuring parameter of the watermarked image (NC, Q, SNR, PSNR, and SSIM) are acceptable are par tradeoff among the imperceptibility, robustness, and number of watermark insertion. The quality of the image is much significant that lie between

Table 8 Parameters values of watermarked image after Gaussian noise attack with variance from 0.001 to 0.004 and extracted watermarks

Variance	NC of Image	Q of Image	PSNR of Image	Extracted Watermarks
0.001	0.99984	0.99878	44.24527	
0.002	0.99892	0.99812	42.74581	
0.003	0.99742	0.99754	40.15497	
0.004	0.99685	0.99647	38.92457	

.99994 to .99998 and SSIM reported from .94 to .99. Whereas the PSNR of the proposed scheme lies between 56.76 to 57.28 db and NC values lie between .9993 to .9998. which shows that the results are better than the existing schemes where PSNR is lies between 32.66 to 52.02 db. After the compression of PSNR and NC values of the proposed scheme with existing schemes (Zairi et al. [37], Takore et al. [31], BW & Permana [34], Thanki et al. [33], Hsu et al. [15], Goli & Naghsh [13], Ernawan et al. [8], Awasthi et al. [3]) we observed that the outcomes are more significant. The proposed scheme is robust against the various noise attacks and JPEG compression. Further, the comparison of the outcomes of the proposed scheme with the existing scheme showed that the performance proposed scheme better than the existing schemes. In this scheme first slice of the NIFTI image (NIFTI images have various numbers of slices) is used for the watermarking to authenticate the NIFTI image. If someone wants to insert watermark in more than one or all slice of the image, then this scheme can be applied on each slice of NIFTI image which he/she want to use for the authentication purpose. Thus, the proposed watermarking scheme can be used for the authentication and identification of the appropriate medical image for the diagnosing of CT-Scan and MRI image in NIFTI images format.

References

1. AHN CJ (2008) Parallel detection algorithm using multiple QR decompositions with permuted channel matrix for SDM/OFDM. *IEEE Trans Veh Technol* 57(4):2578–2582
2. Alshanbari HS (2020) Medical image watermarking for ownership & tamper detection. *Multimed Tools Appl*:1–16
3. Awasthi Y, Sharma A, Pandey R (2019) Image watermarking using APDCBT in selected pixel blocks. In: *2019 8th international conference system modeling and advancement in research trends (SMART)*. IEEE. pp. 250-255
4. Balasamy K, Suganyadevi S (2020) A fuzzy based ROI selection for encryption and watermarking in medical image using DWT and SVD. *Multimedia tools and applications*, 1-20.
5. Chamlawi R, Khan A (2010) Digital image authentication and recovery: employing integer transform based information embedding and extraction. *Inf Sci* 180(24):4909–4928
6. Darwish SM, Hassan OF (2020) A new colour image copyright protection approach using evolution-based dual watermarking. *J Exp Theor Artif Intell*:1–23
7. Daubechies I, Sweldens W (1998) Factoring wavelet transforms into lifting steps. *J Fourier Anal Appl* 4(3): 247–269
8. Ernawan F, Ariatmanto D, Firdaus A (2021) An improved image watermarking by modifying selected DWT-DCT coefficients. *IEEE Access* 9:45474–45485
9. Fan W, Chen J, Zhen J (2005) Spiht algorithm based on fast lifting wavelet transform in image compression. In: Hao Y, Liu J, Wang Y-P, Cheung Y-m, Yin H, Jiao L, Ma J, Jiao Y-C (eds) *Computational Intelligence and Security*. Springer, Berlin, Heidelberg, pp 838–844. https://doi.org/10.1007/11596981_122
10. Fazli S, Moeini M (2016) A robust image watermarking method based on DWT, DCT, and SVD using a new technique for correction of main geometric attacks. *Optik - Int J Light Electron Optics* 127(2):964–972 ISSN 0030-4026
11. Gao T-G, Gu Q-L (2007) Reversible watermarking algorithm based on wavelet lifting scheme," *2007 international conference on wavelet analysis and pattern recognition*, Beijing, pp. 1771-1775.
12. Garg P, Kishore RR (2020) Optimized color image watermarking through watermark strength optimization using particle swarm optimization technique. *J Inform Optim Sci* 41:1499–1512
13. Goli MS, Naghsh A (2017) Introducing a new method robust against crop attack in digital image watermarking using two-step sudoku. In: *2017 3rd international conference on pattern recognition and image analysis (IPRIA)*. IEEE. pp. 237-242
14. Gong LH, Tian C, Zou WP, Zhou NR (2020). Robust and imperceptible watermarking scheme based on canny edge detection and SVD in the contourlet domain. *Multimedia tools and applications*, 1-23.

15. Hsu LY, Hu HT, Chou HH (2019) A blind robust QR code watermarking approach based on DCT. In: *2019 4th international conference on control, robotics and cybernetics (CRC)*. IEEE, pp. 174–178
16. Kaur G, Agarwal R, Patidar V (2020) Crypto watermarking of images for secure transmission over cloud. *J Inf Optim Sci* 41(1):205–216
17. Khalil OH, Elhadad A, Ghareeb A (2020) A blind proposed 3D mesh watermarking technique for copyright protection. *Imag Sci J* 68(2):90–99
18. Lin N, Shen J, Guo X, Zhou J (2011) A robust image watermarking based on DWT-QR decomposition. *2011 IEEE 3rd International Conference on Communication Software and Networks*, Xi'an, pp. 684–688. <https://doi.org/10.1109/ICCSN.2011.6014360>
19. Loukhaoukha K, Chouinard JY, Taieb MH (2010) Multi-Objective Genetic Algorithm Optimization for Image Watermarking Based on Singular Value Decomposition and Lifting Wavelet Transform. In: Elmoataz A, Lezoray O, Nouboud F, Mammass D, Meunier J (eds) *Image and Signal Processing. ICISP 2010. Lecture notes in computer science*, vol 6134. Springer, Berlin, Heidelberg. https://doi.org/10.1007/978-3-642-13681-8_46
20. Ma J, Cheng G, Yixin W, Xingle A, Jiantao G, Ziqi Y, ... He J. (2020) COVID-19 CT lung and infection segmentation dataset (version Verson 1.0) [data set]. Zenodo. <https://doi.org/10.5281/zenodo.3757476>
21. Malini S, Moni RS (2015) Image Denoising using multiresolution singular value decomposition transform. *Procedia Comput Sci* 46:1708–1715
22. Mehta R, Rajpal N, Vishwakarma VP (2016) LWT- QR decomposition based robust and efficient image watermarking scheme using Lagrangian SVR. *Multimed Tools Appl*, ISSN 1380–7501 75:4129–4150
23. Musanna F, Dangwal D, Kumar S, Malik V (2020) A chaos-based image encryption algorithm based on multiresolution singular value decomposition and a symmetric attractor. *Imag Sci J* 68(1):24–40
24. Ni R, Ruan Q, Liu J (2006, November) Tampering estimation watermarking based on lifting wavelet and chaotic sequence. In: *2006 8th international conference on signal processing* (Vol. 4). IEEE
25. Ni R, Ruan Q, Liu J (2006) Tampering estimation watermarking based on lifting wavelet and chaotic sequence. *2006 8th international Conference on Signal Processing*, Beijing, pp.
26. Rahim T, Khan S, Usman MA, Shin SY (2020) Exploiting de-noising convolutional neural networks DnCNNs for an efficient watermarking scheme: a case for information retrieval. *IETE Tech Rev*:1–11
27. Siddharth S, Singh R, Siddiqui TJ (2016), "MSVD Based Image Watermarking in NSCT Domain. In: *2016 Fourth International Conference on Parallel, Distributed and Grid Computing (PDGC)*, IEEE, pp. 685–688, 2016
28. Sree Sharmila T, Ramar K (Oct 2014) Efficient analysis of hybrid directional lifting technique for satellite image denoising. *SIViP* 8(7):1399–1404
29. Su Q, Niu Y, Wang G, Jia S, Yue J (2014a) Color image blind watermarking scheme based on QR decomposition. *Signal Process* 94(1):219–235
30. Sunesh, Kishore RR, Saini A (2020) Optimized image watermarking with artificial neural networks and histogram shape. *J Inform Optim Sci* 41:1597–1613
31. Takore TT, Kumar PR, Devi GL (2016, March) A modified blind image watermarking scheme based on DWT, DCT and SVD domain using GA to optimize robustness. In: *2016 international conference on electrical, electronics, and optimization techniques (ICEEOT)*. IEEE, pp. 2725–2729
32. Thanki R, Kothari A (2020) Multi-level security of medical images based on encryption and watermarking for telemedicine applications. *Multimedia tools and applications*, 1–19.
33. Thanki R, Borra S, Dwivedi V, Borisagar K (2017) An efficient medical image watermarking scheme based on FDCuT–DCT. *Eng Sci Technol Int J* 20(4):1366–1379
34. Tjokorda Agung BW, Adiwijaya, Permana FFPF (2012, July). Medical image watermarking with tamper detection and recovery using reversible watermarking with LSB modification and run length encoding (RLE) compression. In: *2012 IEEE international conference on communication, networks and satellite (ComNetSat)*. IEEE, pp. 167–171
35. Vinothini K, Mydhili S, Periyannayagi S, Sukanya G (2019) Dual watermarking in tele-radiology using DWT for data authentication and security. In: *Proceedings of the 8th IEEE international conference on communication and signal processing*, India, pp. 887–891.
36. Wang Z, Bovik AC (2002) A universal image quality index", *IEEE Signal Processing Letters*, XX
37. Zairi M, Boujiha T, Abdelhaq O (2020, March) An algorithm for digital image watermarking using 2-level DWT, DCT and QR decomposition based on optimal blocks selection. In: *Proceedings of the 3rd international conference on networking, information systems & security*. pp. 1–4